Fourth International Symposium on Marine Propulsors
smp'15, Austin, Texas, USA, June 2015

PLEASE USE 8.5"x11" paper size

Towards Practical Design Optimization of Pre-Swirl Device and its Life Cycle Assessment

Yan Xing-Kaeding, Scott Gatchell and Heinrich Streckwall

Hamburg Ship Model Basin, HSVA
Bramfelder Straße 164, D-22305 Hamburg, Deutschland / Germany

ABSTRACT

Within the EU FP7 project GRIP (Green Retrofitting through Improved Propulsion), HSVA has performed the hydrodynamic design of a Pre-Swirl Stator (PPS) for a bulk carrier. The complete design, optimization and evaluation procedure has been conducted in full scale. The in-house RANS code ***FreSCo***$^{+}$ was coupled with the in-house propeller code QCM (Quasi-Continuous Method) to investigate the complex interaction of hull-ESD-propeller. The resulting PSS design has been constructed and installed on an actual built bulk carrier. Extensive sea trials of this ship without and with PSS have been performed in short sequence and both in good weather conditions. The trial results of a reduction of nearly 7% on power at equal speed (16kn) or an increase of 0.3 kn on speed at equal propulsion power confirmed the effectiveness of the PSS. The actually installed PSS geometry has been measured via 3D laser scan technique and CFD predictions based on the measured geometry are compared to the sea trial results with good agreement. Since the PSS has been designed for a single design condition, a further step has been taken to examine it against off-design conditions to assess the life cycle performance of such a device.

Keywords

Energy Saving Device, ESD, Pre-swirl stator, PSS, CFD, RANS-BEM coupling, Full scale, Hub vortex, Cavitation Reduction

1 INTRODUCTION

On the background of the rapidly increasing fuel oil costs and the international legislation becoming effective to reduce the air pollutions from ships, major European maritime stake holders started a number of research activities to aid the industry to meet the required environmental goals as well as cut costs related to fuel consumption in shipping. The GRIP (Green Retrofitting through Improved Propulsion) project is one of the answers by the EU's 7th Framework of research program in addressing energy efficiency and environmental aspects.

The aims of GRIP is to give ship owners a sound basis of the choice of Energy Saving Devices (ESDs) and further to give more insight into the detailed requirements on the device design by performing an analysis of the hull-ESD-propeller interaction and the structural integrity of the device. The GRIP project such addresses the urgent need from industry for retrofitting ESD solutions for existing ships.

The fact, which makes GRIP project really special and strongly practice-oriented, is that an actual ESD design and its installation for retrofitting scenario and validation sea trials (prior to and after the ESD installation) have been planned and actually performed in this project. HSVA has participated in this activity through designing a Pre-Swirl Stator (PSS) for the full scale validation vessel, which is a 52,000 DWT handymax bulk carrier recently built by the project partner Uljanik shipyard. The PSS designed by HSVA was selected to be installed and tested on the validation bulk carrier. This paper reports on these works mainly in view of three aspects: PSS hydrodynamic design and optimization process, its evaluation and validation of CFD predictions using sea trial results and finally its life cycle assessment.

2 Computational Methods

The baseline of the computational methods applied for ESD final evaluation in this paper is the state-of-the-art RANS method. Though the option to model the propeller in RANS directly has been available and tested, the more practical approach in simulating the propeller effect through body forces as source terms in RANS method has been applied for a quick evaluation of ESD design variants. The body forces are obtained from a Boundary Element Method (BEM), which is coupled iteratively to the RANS method to enable numerical self-propulsion simulations. The propeller analysis and the initial design of PSS have been performed using a BEM approach, taking advantage of its quick response time and low cost. More details of these methods are explained below.

2.1 RANS Method

The HSVA in-house code FreSCo+ is a finite volume fluid flow solver developed in cooperation with the Institute of Fluid Dynamics and Ship Theory (FDS) of the Hamburg University of Technology (TUHH) and the Hamburg Ship Model Basin (HSVA).

The FreSCo+ code solves the incompressible, unsteady Navier-Stokes-equations (RANSE). The transport equations are discretized with the cell-centered finite volume method. Using a face-based approach, the method is applied to fully unstructured grids using arbitrary polyhedral cells or hanging nodes. Also features such as sliding interface or overlapping grid technique have been implemented into the code.

The governing equations are solved in a segregated manner, utilizing a volume-specific SIMPLE-type pressure correction scheme to satisfy the continuity equation, see Ferziger, J.H. and Peric, M. (2002). To avoid an odd-even decoupling of pressure and velocity, a third-order pressure smoothing is employed along a route outlined by Rhie & Chow (1983). The fully-implicit algorithm is second order accurate in space and time. The approximation of the integrals is based on the mid-point rule. Diffusion terms are approximated using second-order central differences, whereas advective fluxes are approximated based on blends between high-order upwind-biased schemes (e.g. QUICK), first order upwind and second order central differences schemes. The latter are applied in scalar form by means of a deferred-correction approach.

Various turbulence-closure models are available with respect to statistical (RANS), such as k-ε (Standard, RNG, Chen), k-ω (Standard, BSL, SST), Menter's One Equation model and the Spalart-Allmaras turbulence model. In this paper, the k-ω SST has been mainly used.

2.2 Propeller Vortex Lattice Method QCM

The method implemented in the "QCM" code is a vortex lattice method (VLM). The blades of the propeller are reduced to lifting surfaces which account for camber and angle of attack. The lifting surfaces are built up by section mean lines. The thickness effect is accounted for by prescribed source densities on the lifting surfaces.

To calculate the load distribution on a lifting surface, a system of rectilinear vortices is introduced. This system is further divided into 'bound' vortices in span wise direction and 'shed' vortices in chord wise direction. This procedure can be considered as a special type of Boundary Element Method. The solution technique follows the standard procedure of boundary element methods in hydrodynamics: The prescribed normal component of the inflow velocity has to be compensated by the downwash due to the vortex system. Demanding this kinematic condition for a set of control points one gets a system of linear equations. From this system the strength of every rectilinear bound vortex is calculated. The system of vortices of known strength is then sufficient to derive the pressure and the forces on the blade surfaces. The typical vortex structure in the propeller wake in QCM is illustrated in Figure 1.

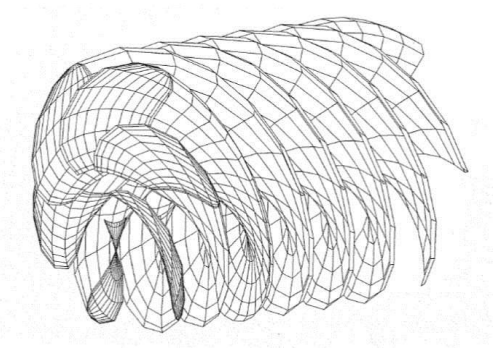

Figure 1: Vortex structure in the propeller wake in QCM for a typical propeller in a homogeneous inflow

The current method is similar to the approaches published by Kerwin and Lee (1978), Greeley and Kerwin (1982) and Nakamura (1985). The chord wise arrangement of corner-points of the vortex–lattice is set up by the 'Cosine-Spacing' as originally recommended by Lan (1974). The results for the loading distribution become identical with the exact solutions of the continuous theory for 2-dimensional thin profiles. Due to this property the method has been named 'Quasi-Continuous Method' (QCM). By using QCM, Nakamura (1985) calculated open water characteristics of various propellers that were in good agreement with experimental results, and established a method for estimating open-water characteristics of unconventional propellers, e.g. contra-rotating, controllable pitch and tandem propellers. Chao and Streckwall (1989) have compared the calculations with other theoretical methods and measurements, also showing a good agreement.

2.3 BEM Propeller Code PPB

The PSS design has been initiated using a BEM method. This method represents a conversion of the propeller analysis program 'PPB'. The conversion work profited from the similarity of stator fins and propeller blades. The potential based BEM propeller code PPB is described in Streckwall (1998). It reflects the true outer surface of the blades using surface panels for discretization. In general the potential based approach is a suitable interpretation of Greens' identity. Applying this identity one obtains an equation for the flow potential disturbance $\Delta\phi_S$ on a surface of concern S. $\Delta\phi_S$ is counted from an undisturbed flow potential ϕ_∞. After obtaining the disturbance $\Delta\phi_S$ the flow variables of interest can be derived. For example the

disturbance of the velocity field $\Delta\vec{v}_S$ (required to deduce the surface pressures) needs a numerical differentiation according to $\Delta\vec{v}_S = -\vec{\nabla}(\Delta\phi_S)$. In the propeller case we use a mixture of hexahedral and triangular panels, whereby the row of trailing edge panels is strictly triangulated. The latter procedure enhances the quality of the surface pressure at the trailing edge and gives a straight forward fulfillment of the Kutta condition.

2.4 Numerical Self-Propulsion using RANS-QCM Coupling

The ESD design and evaluation have been performed using a RANS-QCM coupling approach to simulate a numerical propulsion test. Since it is assumed that the effect of the free surface deformation on ESD performance is negligible, the double body (DB) assumption has been applied together with an additional force (later explained) which represents the missing wave resistance to get the appropriate propeller working condition. To this end the code FreSCo+ is coupled with QCM for propeller analysis in an iterative fashion as outlined in Figure 2.

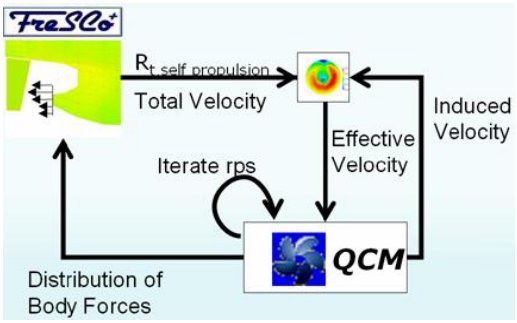

Figure 2: Numerical Propulsion Test Scheme

At the start of the simulation, a nominal wake distribution is extracted from the converged RANS solution without the propeller effect. This velocity distribution and an estimated turning rate are used as an input for the QCM code to compute the forces on the propeller blades (thrust and torque). The turning rate is adjusted until the propeller thrust required to overcome the ship resistance (in propulsion mode) is obtained. The hydro-dynamic forces of the propeller are converted in the form of 3D body forces (source terms) assigned to cells which are representing the propeller disk.

The resulting distribution of the body forces is used as an input to a next RANS calculation loop. The RANS computation is continued in the next iteration cycle and a new total velocity field is created. The propeller induced velocities of the previous cycle, which are an output of the QCM code, are subtracted from the total velocity field. The resulting effective wake distribution is used as input in the subsequent QCM calculation. The iteration is repeated until the equilibrium between the resistance of the ship under self-propulsion condition and the propeller thrust is reached.

3 PSS Hydrodynamic Design and Optimization Procedure

The design procedure of the Pre-Swirl Stator by HSVA is made of four main steps, as illustrated in Figure 3:

1. RANS computation to obtain the wake field at the pre-selected PSS positions
2. BEM optimisation to obtain the optimal twist and camber of the PSS
3. Creation of parametric model for ESD
4. RANS Self-Propulsion computations/optimisations to evaluate the PSS design

In the following, each step will be explained in more details.

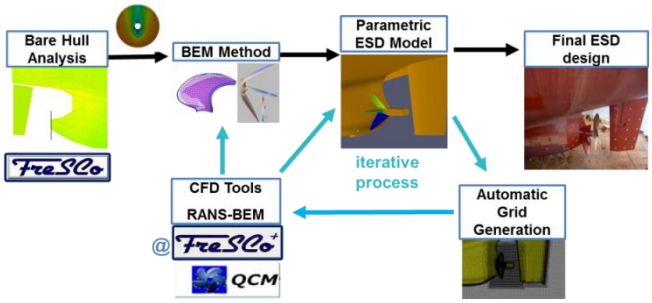

Figure 3: ESD design and optimization procedure at HSVA

3.1 RANS Computations

The DB resistance computation without propeller effect will be computed first for the case without ESD. The result of this simulation gives a first estimation on the possible effect by adding a pre-swirl device onto the hull.

After the resistance computation converges, the so-called numerical propulsion computation can be run either in self-propulsion mode or with a given thrust or rpm of the propeller at an appropriate propeller working point. The requested wake fields for further optimization of PSS in BEM can then be obtained at different pre-defined positions.

Once a PSS has been designed, one may first simulate its interaction with the hull in the resistance mode. It is well known that for a right-hand single-screw ship the propeller rotates in the same direction on the port side as the inward directed tangential component of the inflow. This wake velocity reduces the effective tangential inflow velocity on the blade section resulting in a so-called propeller slip loss (effectively a reduction of rotation rate) that leads to lower thrust on the port side and increases the overall inhomogeneity for the accelerated flow behind the propeller. The tangential velocity component in the wake on

the port side is especially dominant for high block coefficient ships such as tankers or bulkers; by reducing this tangential velocities or even changing its direction from positive to negative through installation of a pre-swirl device, a positive effect in propeller performance could be expected. Such an example is shown in Figure 4.

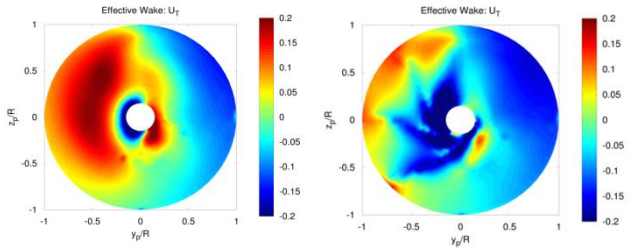

Figure 4: The nominal tangential wake of a bulk carrier: without ESD (left) and with a PSS (right)

3.2 BEM Optimization

The BEM optimization of a PSS starts with a BEM-analysis of the propeller using the PPB introduced before.

The propeller analysis is done first based on the full scale nominal wake calculated earlier using RANS. The circumferential averaged propeller blade circulation is the main target of these propeller calculations. From this blade circulation we derive a shape function which is to be met later by the PSS fins' circulation.

The BEM optimization invoked for the upstream fins requires also an input flow field from RANS (described in previous section) with the propeller effect included. The RANS simulation reflects the geometrical details of the stern bulb at the fins' plane. In the panel system only an idealized hub is modeled, where the roots of the fins are mounted.

The fins' prescribed geometrical data are usually outline, thickness and section type. Other data like camber and angle of attack are modified parameters. Ideally the fins' circulations individually have to meet the above mentioned shape function derived from the propeller analysis. It has however to be kept in mind, that the flow around the fins should be 'sound' which is checked via the BEM results for the fins' surface pressure. A flat suction side pressure distribution is envisaged.

Such derived and properly clustered fins should provide the most reasonable changes to the tangential flow at the propeller as illustrated in Figure 4, so that rotational losses at the propeller and load variations of the propeller blade are best compensated. However, a sound evaluation of the PSS designs is not possible within a BEM method. Further confirmation computations in RANS are necessary for the final PSS adjustment to maximize the improvements.

3.3 Parametric Model of ESD

The parametric models of ESDs applied in this work are generated using the CAD and optimization software FRIENDSHIP-Framework. The ESD parametric models were built up using typical geometrical parameters, such as section profile, angle of attack, extrusion path and scaling of chord etc. Each of these parameters can be selected as design variable.

The output from this parametric model is a watertight, triangulated solid geometry. Figure 5 shows such an example using the parameters described above. This geometry may then be combined with a ship and the general computational boundaries to create the final description of the entire computational domain. This domain is then exported for the subsequent mesh generation stage.

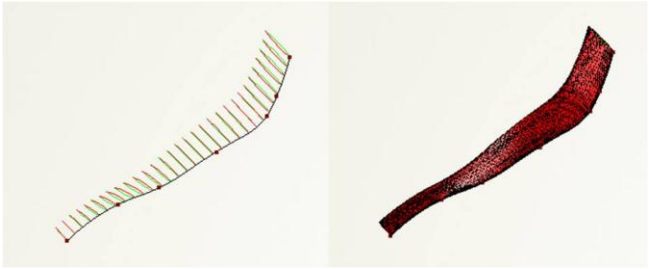

Figure 5: Many Sections along Extrusion Path (left), Lofted Surface (right)

3.4 Evaluation of ESD Designs

Generally, an algorithm is needed to evaluate different ESD designs and compare them with the bare hull case without an ESD. The most direct way to do this is to compare the predicted delivered power at the self-propulsion conditions for ship without and with one or more ESDs installed. The less direct way in judging different designs is to compare the local variables and flow quantities, such as changes in resistance on the hull, resistance/thrust on the ESD, propeller performance/efficiency, rotational/total energy behind the ship etc. The indirect way has certain risk that some of the effects brought by the ESD could possibly be overweighed against other effects, so that the comparison might not be fair for all the designs. Since most of the computations are performed in self-propulsion conditions, the direct way has mainly been employed to evaluate the performance of different designs.

Power Analyses Procedures

Since DB computations have been performed, we need to add a certain force on the hull to correctly evaluate the ESD performance. This force balances the system and makes the propeller working under a proper/reasonable loading corresponding to the most likely operational condition of the propeller. If the computations are performed in full

scale, this force would effectively represent the wave resistance, the air resistance and resistance due to hull roughness. When the computations are performed in model scale, this force would also include the so-called "friction deduction" force to balance the scale effect on frictional forces.

As it is stated before, this additional force is only necessary to obtain a proper/reasonable propeller loading in the coupled analysis. It is actually not required to derive it exactly, apart from the challenge of doing so itself. It is also expected that the performance of the ESD should not vary significantly when the propeller loading changes slightly.

There are different reasonable ways in integrating this force. One of them is introduced below: If the propeller design rpm or thrust from model test is known previously, it can be taken to perform a propulsion computation using the fixed rpm for the base case without an ESD. Then this force can be derived from the expression:

$$F\_unbalanced = T - RT_P \quad (1)$$

T is the total thrust produced by the propeller; RT_P is the total resistance of the ship in propulsion condition.

Then the same force can be applied to all the following self-propulsion computations with ESDs. In this way, the ESD designs can be compared to each other and also to the case without an ESD. If some power gain can be observed, the ESD would prove to work in principle, the higher the power gain ratio, the better the ESD design.

Performance Analyses Procedures

We could consider each pre-stream device (pre-duct or pre-swirl stator), which is attached to the hull, as a wake improvement device. The effect of the ESD would be similar as to provide an optimal aft-hull in this sense. The wake behind the ship can basically be improved in two ways: to accelerate the axial flow where it was too slow or to transform the tangential flow where it was unfavorable. Both measures would make the propeller working more optimal and homogeneous. The objective of a pre-swirl stator would be the latter, producing the pre-swirl where it is needed for the propeller to make the propeller loading more homogeneous and to minimize the rotational losses in the slipstream while keeping the incoming axial wake largely unchanged.

To achieve an overall gain, the propeller performance efficiency behind the ship must be increased with mounted ESD, which can be calculated using

$$\eta_p = \frac{TV_S}{2\pi nQ} = \frac{K_T}{K_Q}\frac{J_S}{2\pi}. \quad (2)$$

The increase of η_p is necessary, but not sufficient. Normally, the overall hydrodynamic efficiency can be expressed as

$$\eta_D = \frac{P_E}{P_D} = \frac{R_T V_S}{2\pi nQ} = \frac{TV_S}{2\pi nQ}\frac{R_T}{T} = \eta_p(1-t). \quad (3)$$

This equation can well explain the difficulty in designing an effective ESD to the hull: an ESD should in principle increase the overall hydrodynamic efficiency with RT taken from the bare hull case. As explained before, a reasonably designed PSS can normally increase the propeller efficiency by enhancing the tangential inflow (e.g. producing pre-swirl) to the propeller. However, due to the inherent working principle of producing pre-swirl, added surfaces (higher frictional resistance) and reduction of the forward propeller clearance to the hull, the required thrust would normally also increase, which would result into an increased thrust deduction. Therefore, a good PSS design would have to provide a favorable balance between these two aspects.

4 RESULTS and DISCUSSIONS

4.1 Full Scale Validation Ship and Its Operational Profile

The selected full scale validation ship is the ship named "VALOVINE", a newly built Bulk Carrier by project partner Uljanik shipyard. The ship is a handymax bulk carrier with its main dimensions of 182 m Lpp, 32 m overall beam and 11 m design draft. Figure 12 shows a photograph of this ship. It is equipped with a conventional Fixed Pitch (FP) propeller of 5.8 m diameter and a d/D ratio of 14.8%. The propeller has 4 blades and rotates right handed. The main design condition of this ship has been defined at the design speed of 15 knots at the design draught by the Uljanik yard with the propeller revolution of 123 rpm. The estimated operational profile can be found in Table 1.

Figure 6: Picture of the bulk carrier "VALOVINE"

Operational Profile	Days per year	Percentage
Ship at sea loaded (design)	165	45.2%
Ship at sea ballast	45	12.3%
Ship berthed	105	28.8%
Ship on anchor	50	13.7%

Table 1: Operational profile of the Uljanik bulk carrier

4.2 Concept Design and Analysis of PSS

Following the design procedure described earlier, HSVA has carried out the pre-swirl stator design and optimization for the validation bulk carrier. In the following, the computational aspects, PSS designs and their evaluations during the concept design phase will be discussed.

Numerical Settings

The DB numerical grids for the cases without and with PSS have about 7.6 M cells and 10.8 M cells, respectively. For cases without and with ESD, the same refinement has been applied to minimize the effects of the grid resolution on the evaluation of an ESD. The numerical gird with PSS is shown in Figure 7 as an example. The boundary conditions and domain sizes are illustrated in Figure 8. The k-ω SST turbulence model has been used and wall functions have been applied to the hull, rudder and ESD in the simulations.

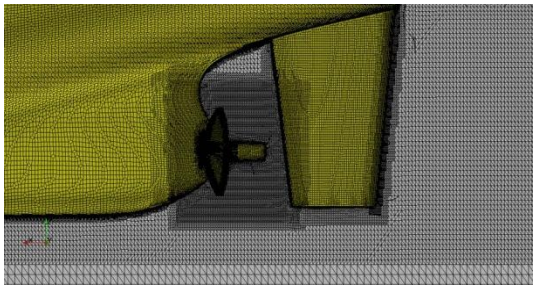

Figure 7: The numerical gird with PSS

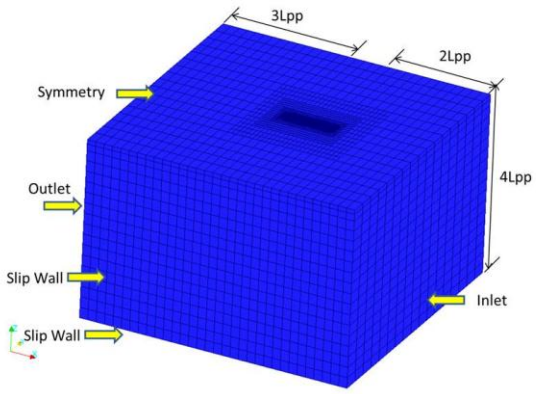

Figure 8: The computational domain and boundary conditions

ESD Designs

As the first step, BEM analysis for the propeller alone has been performed to obtain the circumferential averaged propeller blade circulation. Since it is not clear how many stator fins would actually be optimal to produce enough pre-swirl for the propeller and simultaneously not largely increasing the required thrust (this would probably diminish the gain in propeller performance), two versions were considered: three stators on port side with (V01) and without (V02) starboard stator blade.

The example for the resulting normalized circulation at fins plotted over span can be seen in Figure 9 for PSS V01 in comparison with time average circulation at one propeller blade. Figure 10 shows the geometry of PSS V01 with three port stators and one starboard stator, whereas the PSS V02 with three port stators only is shown in Figure 11. The only difference between these two versions is the number of stator blades. The subsequent RANS evaluations showed that the PSS V02 performs better in this case. After observing a relatively large tip vortex on the stator fins in the RANS computations, the tips have been rounded off, which resulted in PSS V03, shown in Figure 12.

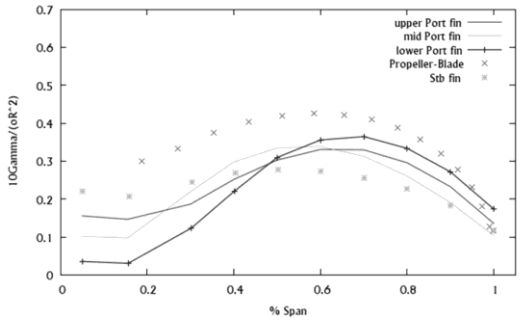

Figure 9: Normalized circulation at stator fins (V01) plotted over span in comparison with time mean circulation at one propeller blade (plotted over radius).

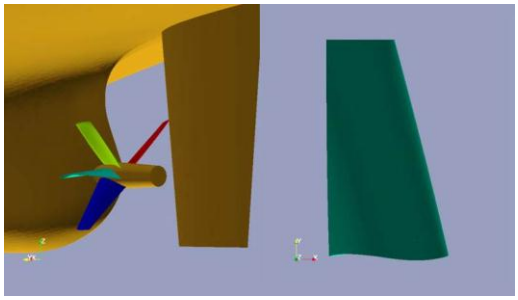

Figure 10: PSS V01 with three port fins and one starboard fin (left) and side view of the fin (right)

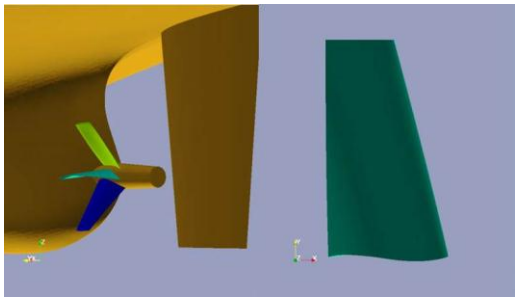

Figure 11: PSS V02 with only three port fins (left) and side view of the fin (right)

During the construction design phase of PSS, it was required to move the root sections of the PSS about 30 cm forward due to structural reasons. There was little time left before the PSS should be actually built so that it was not possible to induce a new PSS design process. This problem

has been solved by introducing some rake to the stator fins so that the sections at higher radii are still experiencing the similar flow field as before. Thanks to the parametric model of the PSS, this change can be easily implemented and the resulted PSS (V04) is shown in Figure 13.

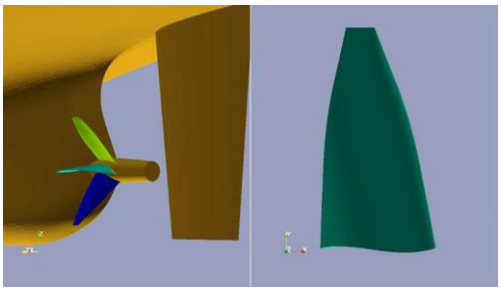

Figure 12: PSS V03 with three port fins only and rounded fin tips (left) and side view of the fin (right)

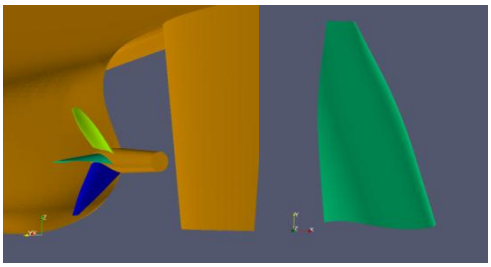

Figure 13: PSS final with three port fins only and rounded fin tips and rake (left) and side view of the fin (right)

RANS Evaluation

The propulsion computation for the bare hull without ESD has been performed first using a constant propeller design rpm, from which the unbalanced force (incl. wave resistance etc.) has been derived. This force has been applied to all the following computations with mounted PSS to make a fair comparison of the energy saving ratios of the different PSS versions.

The self-propulsion computations reflect the change in power requirement due to each PSS directly, which is the top level criterion for the selection of the PSS designs. Figure 14 shows the history of predicted power requirement of PSS design variants in comparison with the bare hull case without PSS. As can be seen, the power requirement has been reduced step by step and the last version is the best design in this case.

To understand why the PSS has actually saved power, a detailed look into flow quantities is necessary. In Figure 15, the computed effective wakes, resulting from the RANS-QCM coupling, are compared between the cases without PSS and with the PSS. The changes in tangential flow due to PSS (Figure 16) shows that the PSS has not only improved the propeller inflow on the port side, but also the starboard side experiences an increased tangential flow which resulted in a higher propeller loading. The corresponding propeller thrust loading distributions are given in Figure 17. The comparison on thrust fluctuation along circumferential direction (Figure 18) between cases without PSS and with PSS variants confirms this conclusion and indicates a more homogeneously loaded propeller when the PSS is installed.

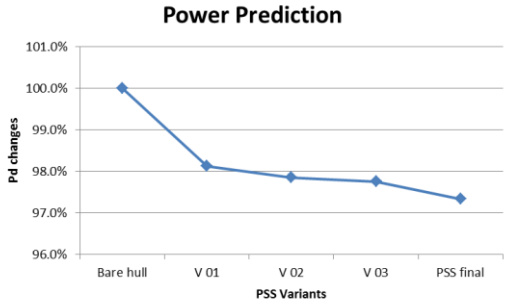

Figure 14: Power gain predictions of the PSS variants

The more detailed force analysis (Figure 19) gives some clue why the PSS V01 does not perform very well. Though the smallest resistance on the hull can be observed among the PSS designs for PSS V01 , the rudder resistance has been increased due to a too high degree of induced pre-swirl, which resulted in attenuating the post-swirl effect of the rudder. Also the starboard fin itself experiences a high resistance, therefore in the later design phase the starboard fin has been omitted. Only the upper fin of V03 is actually producing a small thrust, but all PSS variants in total are producing additional resistance, which means they increase the thrust requirement.

The ESD performance analysis (Figure 20) gives a clearer picture: the PSS V01 with four stator blades has actually increased the propeller performance efficiency most (14.5%), but it is not the best design because the thrust deduction has also been increased by a large amount (11.0%), so that the overall efficiency increase (1.9%) is lowest among the PSS variants. Following this consideration, the following design guideline for the PSS design can be derived: A good PSS design would characterize itself in mainly two aspects: to produce as much pre-swirl as possible to increase the propeller efficiency η_P; to increase the thrust deduction as moderate as possible to reach a best compromise in terms of η_D.

One effect due to a PSS installation, which needs to be pointed out, is a reduction of the rpm (about 5%, can be observed from Figure 20) even when the propeller has to produce higher thrust with the PSS installed. This amount of propeller rotation rate reduction needs to be taken into account when the PSS is retrofitted to an existing ship.

Another effect observed from the PSS is the hub vortex reduction. Figure 21 shows the streamlines passing through the propeller hub region indicating a less strong hub vortex due to PSS. A more detailed look at the pressure distribution on the stern and hub, see Figure 22, confirms

that the pressure drop on the hub, which is normally caused by the presence of the hub vortex, has changed its sign from a negative resistance (less desirable) to a positive thrust (more favorable). When adding the PSS, more pre-swirl has been added to the propeller inflow, not only in the high radius region but also in the root region of the propeller, and the slipstream is especially expected to contain less 'center'-swirl now (even with higher propeller loading), which results in the positive effect of reducing the strength of hub vortex in this case.

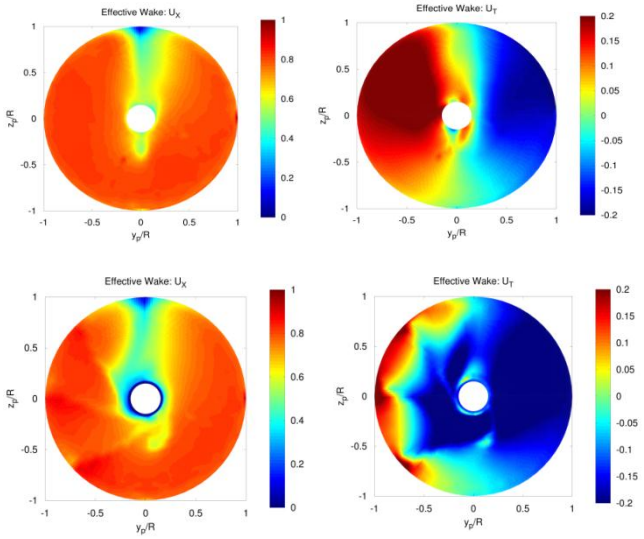

Figure 15: Comparison of effective axial (left) and tangential (right) wakes between cases without an ESD (top) and with PSS final (bottom)

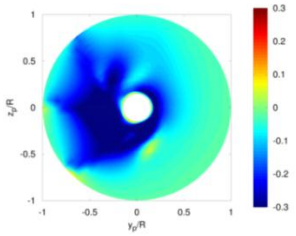

Figure 16: Changes of tangential wake due to PSS

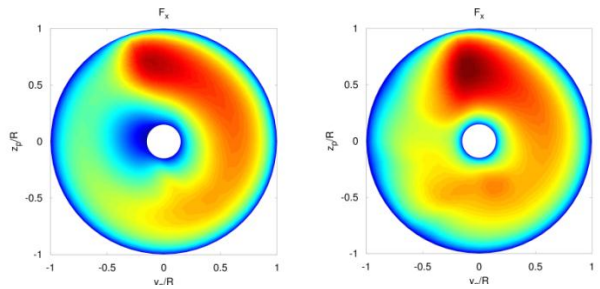

Figure 17: Comparison of Propeller Thrust loading distributions between cases without an ESD (left) and with PSS final (right)

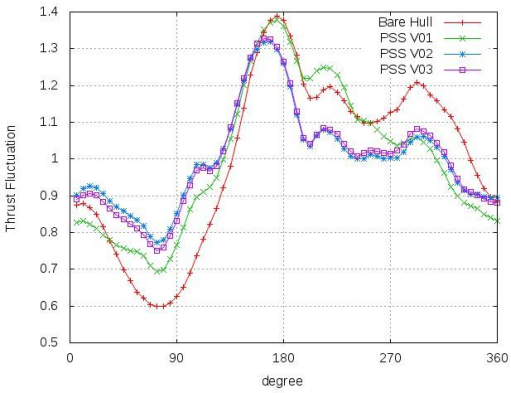

Figure 18: Comparison of thrust fluctuation of along circumferential direction between cases without an ESD and with PSS versions

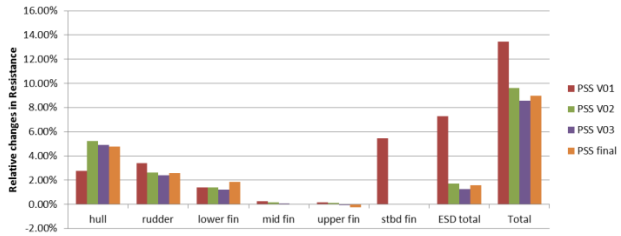

Figure 19: Relative changes in Resistance forces of PSS designs comparing to the bare hull

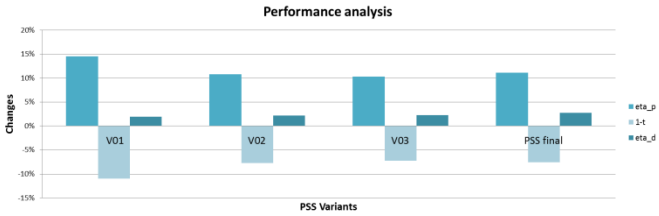

Figure 20: Performance analysis of PSS versions

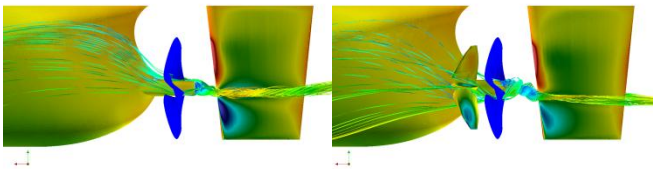

Figure 21: Streamline passing behind the propeller hub together: without ESD (left) and with PSS (right)

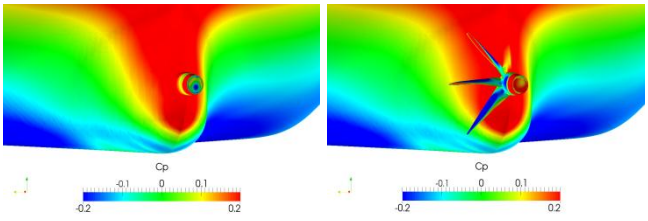

Figure 22: Cp Distribution on the ship stern and the hub: without ESD (left) and with PSS (right)

4.3 Speed Trials without and with PSS

As mentioned before, the PSS fins have been built and installed on the bulk carrier in the dry dock between two speed trials conducted in the Adriatic Sea. The trials were executed following the most up-to-date ITTC procedures (2012) in heavy ballast conditions. Both trials were run under good weather conditions. The hull and Propeller surface conditions were surveyed in the dry dock directly after the first trial. The same strain gauge installed on the propeller shaft has been used for both trials. In general, the measurement uncertainties in wind, wave, draft, speed and power have been estimated to be smaller than 0.7% (see Hasselaar and Xing-Kaeding, 2015). The corrected trial results are shown in Figure 23. As can be seen, 6.8% power saving effect due to PSS has been identified and the propeller rpm reduction is indeed very pronounced, namely 5.2%. Apart from the fuel saving effects, a reduction of the cavitating hub vortex was found through high-speed underwater cavitation observations, which confirms the CFD predictions shown before.

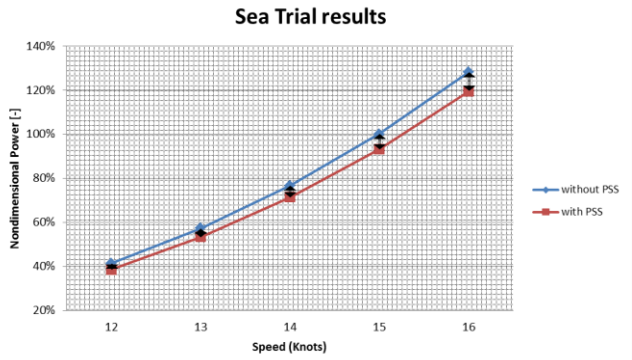

Figure 23: Speed trials results without and with PSS

4.4 Comparison of CFD and Sea Trial

In order to validate the CFD predictions the geometry of the PSS fins – as built - were measured using a 3D laser scan just prior to the second speed trial. It is often found that during manufacturing and installation, the geometry and position of the stator is slightly different from the designed one. The comparison between the original geometry and the one determined by 3D laser scan showed some differences concerning the fins' longitudinal positions, twist and thickness, whereas the angular positions of the fins have been kept very well. Due to the geometrical differences, a direct comparison between the CFD results from the original geometry and the trial results becomes impossible. Therefore, a new CFD mesh based on the 3D in-situ geometry measurement was made.

The numerical mesh generated for the 3D - as built - geometry has 11.2M cells. The new numerical mesh reflects the thickness increase on the pressure sides of the fins which has been changed later due to structural reasons and shows the blunt tips from the building of the fins, see Figure 24. Other numerical settings have been kept identical to the CFD design phase.

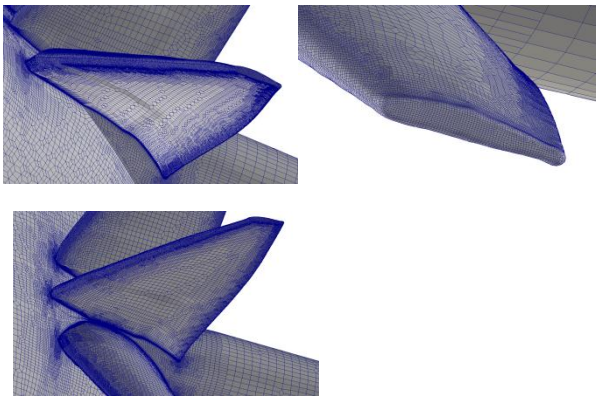

Figure 24: New generated CFD mesh based on the measured in-situ 3D model

The calculated power-speed relations have been compared to the sea trial results for cases without and with the PSS, shown in Figure 25. As can been seen, the trends of both curves have been predicted by CFD very well, however there is still a certain gap in absolute power for both cases without and with PSS. And the effect of the PSS has been somewhat under-predicted by CFD when comparing to trial results.

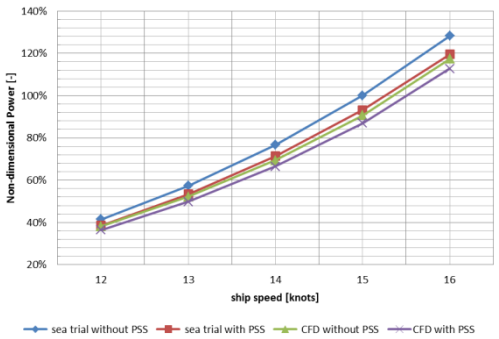

Figure 25: Comparison of predicted power-speed relation with the trial results

Since the propeller rpm has been taken from the trial for the case without the PSS, the under-prediction in power finds its clue directly in under-prediction in propeller torque. Though there might be more sources for this under-prediction of the torque, one physical effect which has not yet been included in the CFD model is the propeller blade roughness. Even for a well-polished propeller, the blade surface is not 'hydrodynamically smooth' as normally assumed in the CFD simulations, when it is operating in full scale (high Rn Regime). Therefore, the blade roughness model has been included in the CFD computations with an assumption of roughness height of 30 μm according to the ITTC method (2000). The differences in results are

noticeable (see Figure 26) and the relative error ranges of the prediction with consideration of propeller blade roughness are given in Figure 27. As can been seen, the deviation of delivered power between CFD prediction and trial results can be reduced when the propeller blade roughness is considered, which is below 8% in the whole speed range.

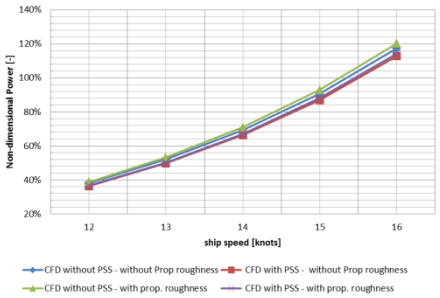

Figure 26: Comparison of predicted power-speed relation without and with considering the propeller blade roughness

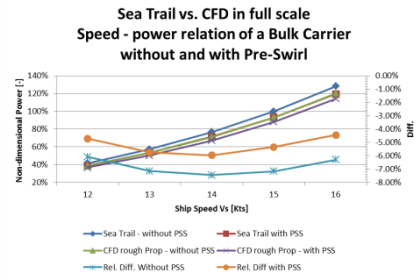

Figure 27: The error range of full scale CFD power prediction with consideration of the roughness of propeller blades

Beside the absolute power prediction, the relative changes of power and rpm due to the installation of the PSS are of more interest in this study. Figure 28 shows the changes of shaft power, the propeller rpm and the torque for one ship speed in sea trial, full scale CFD prediction without and with considering the propeller blade roughness. It shows that the under-prediction of the PSS effect in CFD has also been improved by considering the propeller blade roughness. The CFD prediction in propeller rpm reduction is satisfactory. The errors in prediction of changes in propeller torque seems to be still high, though improvement can also be observed here when the propeller blade roughness is taken into account.

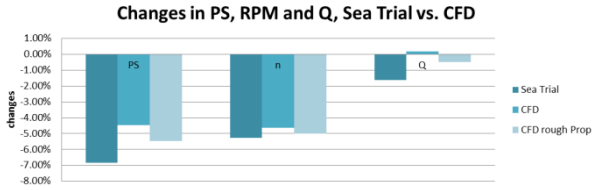

Figure 28: Comparison between sea trial and CFD results on changes of shaft power, propeller rpm and torque due to PSS

4.5 Life Cycle Analysis of PSS

After CFD results have been compared and validated, further evaluation of the ESD in operational conditions have been performed, which enables the engineers to answer the following question: Is the performance of ESDs sensitive to different speed and floating conditions of the ship? This question is of great importance for ship owners when considering whether or not to install a PSS as ships will be operated during their lifetime in numerous conditions different from the design condition originally specified for the vessel. If an ESD is performing well at its design condition but poor at all other conditions, or say, that the performance of an ESD design is very sensitive to ship operating conditions, it would not be a good design for this ship. From the results of such evaluations, ESD fuel saving aspects during the life cycle of a ship can also be derived.

In the section 4.1, the operational profile for the Uljanik Bulk carrier has been introduced and defined. To evaluate the PSS performance at different conditions, the original parametric model of PSS with adaptation to measured geometry has been used with consideration of propeller blade roughness. Numerical meshes with similar mesh density have been generated for the off-design conditions accordingly.

The predicted changes in PD, RPM, Thrust and Torque at different operational conditions are shown in Figure 29. As can be seen, the PSS performs best at the design condition as expected and about one percent worse at both off-design conditions (one of which is identical with the sea trial condition). Both the thrust increase and the rpm reduction are around 5% in all investigated conditions.

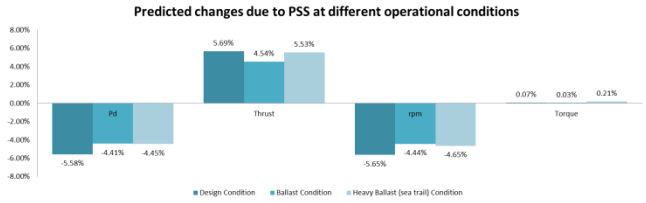

Figure 29: Changes in PD, Thrust, RPM and propeller torque due to PSS at different operational condition

A detailed look at the resistance forces changes on different components in the hull-ESD-propeller system (Figure 29) reveals that the resistances on the hull and rudder have largest increases in case of design condition indicating that the pre-swirl induction effect of the PSS is highest in this case. Also the middle and upper fin seems to produce certain thrust in design condition while this effect diminishes under the off-design conditions, where the angles of attack for the fins are no more optimal. Though the required thrust increase is actually the highest in the design condition the higher pre-swirl effect due to the PSS

leads to a greater rpm reduction and a higher power saving ratio in this case.

Figure 31 shows the normalized resultant total forces (normalized by propeller disk area multiplied by the stagnation pressure) on each fin under different conditions. As can be seen, the resultant forces on all three fins are highest in design condition, which indicates again the highest pre-swirl effect in this case. This is consistent with the pressure distribution on these three fins at different operational conditions, see Figure 32. A more detailed look into the vertical flow at the PSS position (Figure 33) reveals: the oblique/transverse flow has been reduced to a large extent in the off-design conditions. The decrease of the vertical flow in this case will reduce the angles of attack for the PSS fins, which in turn will diminish the pre-swirl generation effect of the PSS. From Figure 32 it can be also seen that the suction area on the middle and lower fins becomes smaller, which results also into an increased resistances of the PSS fins (Figure 30). The reduction of the vertical flow in off-design condition has not only made the PSS work less optimal, but also diminished the level of potential energy losses which an optimal aligned PSS could have recovered.

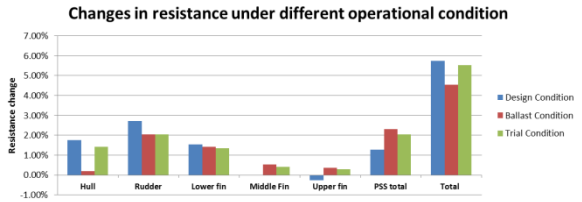

Figure 30: Changes in resistance forces due to PSS at different operational conditions

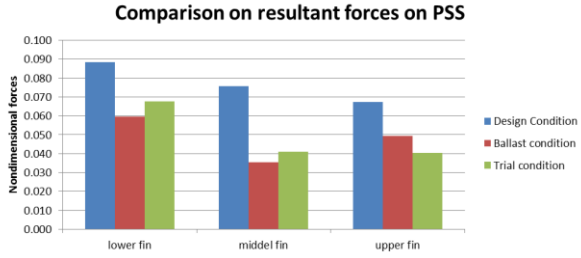

Figure 31: Changes in resultant forces on PSS at different operational conditions

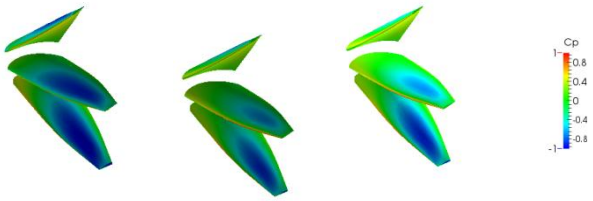

Design Ballast Trial

Figure 32: Pressure Distribution on PSS under different operational conditions

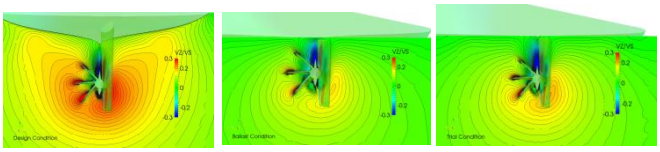

Design Ballast Trial

Figure 33: Inflow Velocity Vz at PSS under different operational conditions

The PSS performance analysis, see Figure 34, confirms that the overall hydrodynamic efficiency increase is highest in the design condition which is mainly caused by the largest propeller performance increase (due to highest pre-swirl generation, see Figure 35) while paying a certain penalty due to the largest increase in the thrust deduction.

In general, the PSS seems to perform quite stable with an averaged 4.5% predicted power saving ratio under the defined operational profile. Assuming the fuel consumption of the main engine being 7000 ton per year, this gives about 315 ton fuel saving per year. Taking an average fuel price (IFO180) of 420$/ton, this would mean 132 k$ saving per year with PSS installed. Considering the retrofitting cost of such a device being 90 k$ (prices are location dependent), the return of investment is accomplished in less than a year, namely 8 months. Not only economically but also ecologically this is a worthwhile investment.

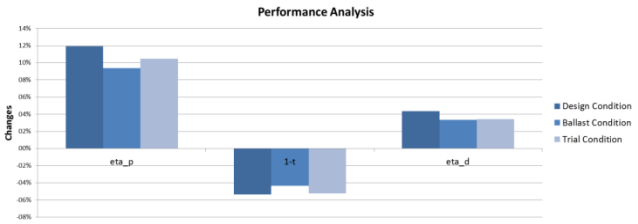

Figure 34: Performance analysis at different operational conditions due to PSS

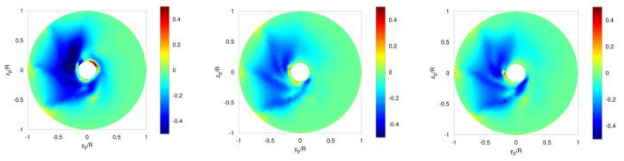

Design Ballast Trial

Figure 35: Changes on tangential effective wake due to PSS under different operational conditions

5 CONCLUSIONS

The hydrodynamic design procedure for Energy Saving Devices (ESDs) developed in the EU FP7 project GRIP has been successfully applied to a newly built 52,000 DWT Bulk carrier by Uljanik shipyard in Croatia. The Pre-Swirl Stator designed by HSVA was selected to be installed on

the validation ship and successfully tested during the trials, which gave a power gain ratio of 6.8%.

The mechanism that leads to a successful power reduction due to a PSS installation was shown to be the generation of pre-swirl and its submission into the propeller plane. This pre-swirl both redirects the resulting force vector on the propeller blades to a higher effective angle of attack such that the thrust/torque ratio of the blade is improved, and reduces the propeller rotation rate needed to deliver the demanded thrust. Both the reduced rotation rate and the improved thrust/torque ratio lead to a reduced power requirement. The decrease in propeller rotation rate due to PSS is about 5% in this case.

The ESD design and evaluation using the RANS-QCM coupling method seems to be an efficient method for the ESD evaluation and optimization process due to its relative low cost and the quick response time. Simultaneously the method seems to be sensitive enough to reflect the flow changes introduced by ESDs.

The measured 3D geometry using laser scan technique and the trial results without and with PSS have been utilized for validation purpose of the full scale CFD simulation. A generally good agreement has been obtained with the absolute power prediction offset below 8% for the whole speed range. The power saving effect by PSS is predicted about 5.3% in average by CFD while 6.8% was measured at sea trials. By considering the propeller blade roughness, an improvement of the CFD power saving prediction of 1% has been observed.

Different operational conditions have been investigated to evaluate the PSS performance and it turned out that the PSS gives positive net gains for all loading conditions, though the highest gain is seen at design condition as expected. In general, the PSS seems to be not very sensitive to the operational conditions of the vessel and, therefore, can be considered as a life cycle adapted design.

ACKNOWLEDGMENTS

This research is partly funded by the European Union under the 7th Framework Programme (FP7) under Grant Agreement 284905. The work reported here would not have been made possible without the support and good collaboration of the project partners. Special thanks are expressed to ULJANIK BRODOGRADILISTE DD, MARIN, ACCIONA Compania Trasmediterranea SA and IMAWIS.

The content of this publication is the sole responsibility of the authors.

REFERENCES

Chao, K. Y. and Streckwall, H. (1989) „Berechnung der Propellerumstroemung mit einer Vortex-Lattice Method“, Jahrbuch der Schiffbautechnischen Gesellschaft, Band 83, 1989

Ferziger, J. H. and Peric, M. (2002) “Computational Methods for Fluid Dynamics”, Springer Verlag, 3rd edition.

Greeley, D. S. and Kerwin, J. E. (1982) “Numerical Methods for Propeller Design and Analysis in Steady Flows”, SNAME Transactions, Vol. 90

Hasselaar. T. W. F. and Xing-Kaeding Y. (2015) “Evaluation of an energy saving device via validation speed/power trials and full scale CFD investigation”, International Shipbuilding Progress, submitted

ITTC. (2012) “Recommended procedures and Guidelines - Speed and power trials Part 1: Preparation and Conduct; Part 2: Analysis of Speed/Power Trial data”, Report No.: ITTC 7.5-04-01-01.2.

ITTC. (2000) “1978 ITTC Performance Prediction method”. Report No.: ITTC 7.5-02-03-01.4.

Kerwin, JE and Lee, C. S. (1978) “Prediction of Steady and Unsteady Marine Propeller Performance by Numerical Lifting-Surface Theory”, SNAME Transactions, Vol. 86

Lan, C. E. (1974) “A Quasi-Vertex-Lattice Method in thin Wing Theory”, (E), J. of Aircraft, Vol. 11.

Nakamura, N. (1985) “Estimation of Propeller Open-Water Characteristics Based on Quasi-Continuous Method”, Joun. Of the Soc. Of Nav. Arch. of Japan, Vol. 157

Rhie, C. M. and Chow, W. L. (1983) “A numerical study for the turbulent past an isolated airflow with trailing edge separation”, AIAA Journall, 17, 1525–1532.

Streckwall, H. (1998) “Hydrodynamic Analysis Three Propellers Using a Surface Panel Method for Steady and Unsteady Flow Conditions”, Proc. 22nd ITTC Propulsion Committee Propeller RANS/Panel Meth. Workshop, Grenoble, France.

DISCUSSION

Question from Dmitriy Ponkratov

1. Was the hull cleaned in dry-dock?
2. Were superstructure/appendages included in the CFD?
3. Was cavitation on PSS assessed by CFD?
4. Were the cavitation observations done by ballast draught?

Authors’ Closure

Thank you for your questions. I would like to answer the questions in the sequence. The bottom part of the hull was indeed pressure-cleaned in the dry-dock. But before cleaning the hull an inspection has been

executed by the trial team. Only minimal fouling can be found on the submerged part of the hull. The vessel has been launched on September 28, 2013 and has been alongside the yard in Croatia until the beginning of April 2014 for outfitting. The development of hull fouling during this period was minimal due to the cold climate (winter) and the first 1/3rd of the vessel, which is most important in terms of frictional resistance, was largely out of the water during outfitting. Primarily the flat bottom was submerged. Due to the lack of sunlight this area the development of bio-fouling in this region is reasonably slow. For more details, there will be one journal paper of Thijs W.F. Hasselaar and me coming out on a special issue of the ISP with the title "evaluation of an energy saving device via validation speed/power trials and full scale CFD investigation".

For the second question, there have been no superstructure/appendages modeled in the CFD, since the main investigations are performed with double body assumptions.

Now to answer the third question: No cavitation on PSS has been addressed by CFD. Only cavitation on propeller due to PSS has been numerically addressed, which seems to give a positive influence.

The trails and cavitation observations are performed on a so-called heavy ballast draught, which is in between the ballast and the design draught.

Question from Neil Bose

Thank you for an excellent presentation of a very thorough study. I have two questions:

1. During the two sea trials held one week apart what other work was done on the ship hull while the fins were fitted?
2. What was the structural design of the fins and how were they fitted?

Authors' Closure

Thank you for your questions. The first question has been partially answered before. During dry dock an assessment was made of the hull fouling, the complete hull was pressure cleaned, the stator fins were installed, docking studs were removed and the flat bottom re-coated. The docking studs, 8 in total measuring approx. 1200x70x50mm were orientated in longitudinal direction. A first estimate indicated negligible resistance from the studs, due to their small height, the developed boundary layer at their location and streamlined alignment. It is not expected that the removal of the studs would therefore influence the ESD performance assessment. The hull was found in good condition with only a very light and invisible (following the superintendent negligible) layer of slime fouling on the flat bottom. No green weed fouling, barnacles or other types of fouling had developed. The propeller remained untouched during the docking.

The structural design and assessment of the fins have been done by project partner Uljanik shipyard and Bureau Veritas. According to BV, the conclusion of the FEM static analysis is that the complete connection of the fin to the stern tube allows to ensure a structural continuity and all strengths go through the hull. Accordingly, no hot spot stress has been observed at the connections, and all computed stresses are below the allowable stresses. For more details, there will be one journal paper of Thijs W.F. Hasselaar and me coming out on the same special issue of the ISP with the title "ESD Structural Issue – Upstream Device" by Stéphane Paboeuf and Antoine Cassez.